

Original Research

# Inhibition of *PFKFB3* Expression Stimulates Macrophage-Mediated Lymphangiogenesis Post-Acute Myocardial Infarction

Tianyi Cui<sup>1</sup>, Chao Feng<sup>2,3,\*</sup>, Hantao Jiang<sup>2</sup>, Ying Jin<sup>2</sup>, Jinping Feng<sup>2,3,\*</sup><sup>1</sup>State Key Laboratory of Modern Chinese Medicine, Tianjin University of Traditional Chinese Medicine, 301617 Tianjin, China<sup>2</sup>Department of Cardiology, Tianjin Chest Hospital, 300222 Tianjin, China<sup>3</sup>Tianjin Key Laboratory of Cardiovascular Emergency and Critical Care, Tianjin Municipal Science and Technology Bureau, Tianjin Chest Hospital, 300222 Tianjin, China\*Correspondence: [fengchao@nankai.edu.cn](mailto:fengchao@nankai.edu.cn) (Chao Feng); [fjptj666@163.com](mailto:fjptj666@163.com) (Jinping Feng)

Academic Editor: Ioanna-Katerina Aggeli

Submitted: 19 April 2023 Revised: 25 July 2023 Accepted: 8 August 2023 Published: 3 November 2023

## Abstract

**Background:** The dilation of lymphatic vessels plays a critical role in maintaining heart function, while a lack thereof could contribute to heart failure (HF), and subsequently to an acute myocardial infarction (AMI). Macrophages participate in the induction of lymphangiogenesis by secreting vascular endothelial cell growth factor C (VEGF-C), although the precise mechanism remains unclear. **Methods:** Intramyocardial injections of adeno-associated viruses (AAV9) to inhibit the expression of *VEGFR3* (*VEGFR3* shRNA) or promote the expression of *VEGFR3* (*VEGFR3* ORF) in the heart; Myh6-mCherry B6 D2-tg mice and flow cytometry were used to evaluate the number of myocellular debris in the mediastinal lymph nodes; fluorescence staining and qPCR were used to evaluate fluorescence analysis; Seahorse experiment was used to evaluate the level of glycolysis of macrophages; *Lyz2<sup>Cre</sup>*, *VEGFC<sup>fl/fl</sup>*, and *PFKFB3<sup>fl/fl</sup>* mice were used as a model to knock out the expression of *VEGF-C* and *PFKFB3* in macrophages. **Results:** The escalation of *VEGFR3* in cardiac tissue can facilitate the drainage of myocardial debris to the mediastinal lymph nodes, thereby improving cardiac function and reducing fibrosis after reperfusion injury. Conversely, myeloid *VEGF-C* deficiency displayed an increase in macrophage counts and inflammation levels following reperfusion injury. The inhibition of the critical enzyme *PFKFB3* in macrophage glycolysis can stimulate the manifestation of *VEGF-C* in macrophages. A deficiency in myeloid *PFKFB3* is associated with induced lymphangiogenesis following reperfusion injury. **Conclusions:** Our initial investigations suggest that the suppression of *PFKFB3* expression in macrophages could potentially stimulate the production of *VEGF-C* in these immune cells, which in turn may facilitate lymphangiogenesis and mitigate the inflammatory effects of I/R injury.

**Keywords:** *PFKFB3*; macrophages; ischemia-reperfusion injury; lymphangiogenesis

## 1. Introduction

Acute myocardial infarction (AMI) represents a substantial danger to human health, attributable to its heightened prevalence and mortality rates [1,2]. Although medication, interventional therapy, and cardiac surgery are commonly employed to treat AMI, incomplete reperfusion, and the existence of extensive or multiple infarcted areas may result in left ventricular (LV) remodeling [1,3]. This process may further aggravate the advancement of heart failure (HF), which is clinically identified as ischemia-reperfusion (I/R) injury [1,3]. The current focus for cardiovascular disease pertains to the suppression of the advancement of ventricular remodeling caused by I/R, and the identification of efficacious therapeutic approaches and targets.

The emergence of therapeutic lymphangiogenesis as a potential solution to reduce inflammation and ventricular remodeling after an acute myocardial infarction has shown promise in preventing the onset of heart failure [4–6]. Recent research has substantiated the advantageous impact of lymphatic vessels in the course of cardiac remodeling [4,5]. Following AMI, the upregulation of vascu-

lar endothelial cell growth factor C (*VEGF-C*) stimulates the expression of lymphatic growth factor, which promotes the development of cardiac lymphatic vessels, and ultimately, improves cardiac function [7]. Additionally, the cardiac lymphatic system is associated with the subsiding of inflammation following myocardial infarction [5]. Notably, CD11b<sup>+</sup> macrophages have been observed to secrete *VEGF-C*, thereby promoting lymphangiogenesis [8,9].

The metabolic reprogramming of macrophages, specifically their adoption of aerobic glycolysis or the Warburg effect, has emerged as a significant mechanism driving the conversion of macrophages into inflammatory phenotypes [10,11]. The PFKFB enzymes are a subset of glycolytic regulators that facilitate the production of fructose-2,6-bisphosphate (F-2,6-P<sub>2</sub>) [12]. The *PFKFB3* isoform is the dominant isoform among the four PFKFB isoforms, and it is primarily expressed in vascular cells, leukocytes, and many transformed cells. Nevertheless, the connection between the aerobic glycolysis of macrophages and lymphangiogenesis, and the regulatory function of *PFKFB3* in this regard, is yet to be fully understood.



The present study elucidates the correlation between macrophage aerobic glycolysis and the expression of *VEGF-C* induced by macrophages. It has been preliminarily established that hampering the expression of *PFKFB3* in macrophages can augment the production of *VEGF-C* in macrophages, thereby facilitating lymphatic neogenesis and the amelioration of inflammatory response after I/R.

## 2. Methods

### 2.1 Animal Use and Study Approval

All animal and surgical procedures conformed to Directive 2010/63/EU, issued by the European Parliament. All animals were handled according to the guidelines of the TCM Animal Research Committee (TCM-LAEC20221178) of Tianjin University of Traditional Chinese Medicine. C57BL/6J mice (20 ± 20 g) were provided by Beijing Vital River Laboratory Animal Technology (Beijing, China). *Lyz2Cre* and *VEGF-C<sup>fl/fl</sup>* mice were provided by GemPharmatech (Jiangsu, China). *PFKFB3<sup>fl/fl</sup>* mice were provided by Shanghai Biomodel Organism Science & Technology Development (Shanghai, China). *Myh6-mCherry B6 D2-tg* mice were obtained from The Jackson Laboratory. Male mice were solely utilized as the animal participants in this study. The animals were housed in a specific-pathogen-free (SPF) animal facility in the experimental animal center of Tianjin University of Traditional Chinese Medicine, under controlled temperature (22 ± 2 °C) and humidity (40 ± 5%), and with a 12 hours light/dark cycle, and received a standard pellet diet with continual access to water.

### 2.2 Transfected and Transgenic Animal Procedures

Specific *VEGFR3* knockdown or overexpression was achieved in the left ventricles of the mice by using adeno-associated viruses-based (AAV9) delivery vectors (Genechem, Shanghai, China). AAV9 expressing the *VEGFR3* open reading frame (titer:  $1.76 \times 10^{12}$ ), *CCR2*-shRNA (titer:  $1.65 \times 10^{12}$ ), or a scrambled control sequence bearing no homology to known gene transcripts (titer:  $1.54 \times 10^{12}$ ) were injected into the left ventricle at multiple sites. After a period of 30 days, the mice were subjected to I/R surgery and subsequent treatments.

### 2.3 Ischemia-Reperfusion (I/R) Models

I/R models were prepared according to our previous studies [13,14], and the left anterior descending coronary artery (LAD) was ligated through the utilization of a 6-0 silk suture. Following a duration of 60 minutes, the suture was removed to facilitate reperfusion. The experimental cohort underwent a procedure involving ligation, whereas the control group underwent a sham procedure that mimicked the experimental intervention, although without the actual ligation. In order to apply the *VEGFR3* inhibitor as a treatment, mice were subjected to an intraperitoneal injection of

MAZ51 at a dose of 10 mg/kg per bodyweight (#676492-10MG, sigma-Aldrich, Shanghai, China), as previously described [15,16].

### 2.4 Cardiac Functional Measurements

Mice echocardiography was performed using a ultra-high-resolution animal ultrasound imaging system (Vevo 2100, VisualSonic, Toronto, IL, Canada) and the left ventricular function was evaluated as previously described [16]. Long axes were observed through the utilization of M-mode imaging. Three representative cycles were captured for each animal, and measurements were performed for ejection fraction (EF%) and fractional shortening (FS%).

### 2.5 Cell Culture

Bone marrow-derived macrophages (BMDM) were procured from bone marrow, utilizing the previously established method [17,18]. The femur bones of the mice were subjected to sterilization via a 10-minute treatment with 75% ethanol, followed by flushing using Iscove's Modified Dulbecco's Medium (IMDM), containing 2% fetal bovine serum (FBS). After treating the red blood cells with red blood cell lysis buffer, the entire solution was centrifuged. Then, the resulting cell pellet was suspended in fresh IMDM containing 10% FBS and 20 ng/mL GM-CSF. Cells were all cultured in a humidified incubator at 37 °C and 5% CO<sub>2</sub>. Cell cultures were replenished with fresh IMDM every third day. After a period of 10 days, the macrophages were acquired. The polarization of macrophages towards M1 can be achieved by subjecting them to 1 µg/mL LPS (Sigma-Aldrich, #L4391-10X1MG) and 50 ng/mL IFN-γ (#APA033Mu61, Cloud-Clone Corp, Wuhan, China) stimulation for a duration of 24 hours. The inhibition of macrophage glycolysis was achieved through the implementation of 3PO (10 µM/L; #HY-19824, MedChemExpress, Shanghai, China). For cell transfections, macrophages were stably transfected with *VEGFR3*-overexpressing lentivirus (Genechem, Shanghai, China) or lentivirus containing scrambled control sequences. Briefly, macrophages were inoculated into 6-well plates and cultured at 37 °C. The infection reagent and lentivirus were added to macrophages for 72 hours, according to the manufacturer's instructions. All cell lines were validated by STR profiling and tested negative for mycoplasma.

### 2.6 Fluorescence-Activated Cell Sorting (FACS) and Flow Cytometry Analysis

For single-cell suspensions, the Multi-Tissue Dissociation Kit 2 (#130-110-203, Miltenyi, Bergisch Gladbach, Germany) and gentleMACS Dissociator device (Miltenyi) were used to dissociate cells from mice hearts. The collected cells were incubated with antibodies at 37 °C for 20 minutes. F4/80<sup>+</sup> macrophages were isolated and purified using a FACSaria II (BD, Franklin Lakes, NJ, USA) flow cytometer. Flow cytometry was performed using a

Flow Cytometer (NovoCyte, Agilent, Santa Clara, CA, USA). Data were analyzed using FlowJo software (Version V10.8; TreeStar, Ashland, OR, USA) and NovoExpress (Version 15.0; Agilent). The antibodies used in this study were anti-mouse CD16/32 (TruStain FcX™, Biolegend, San Diego, CA, USA), CD45 antibody, anti-mouse, APC (#130-123-784, Miltenyi); CD11b antibody, anti-human/mouse, FITC (#130-113-796, Miltenyi); PerCP anti-mouse F4/80 antibody (#123126, Biolegend); Ly6G antibody, PE, eBioscience™, REAfinity™ (#12-9668-82, Thermo Fisher, Waltham, MA, USA); APC/cyanine7 anti-mouse Ly-6C antibody (#128026, Biolegend); FITC anti-mouse CD64 antibody (#161008, Biolegend).

### 2.7 Mitochondrial Respiration and Glycolysis

Extracellular acidification rates (ECARs) were assessed using a Seahorse analyzer (XF96, Agilent), as previously described [19]. Briefly, macrophages were cultured in 96-well plates followed by the sequential addition of 20 mM glucose, 2 μM oligomycin, and 80 mM 2-DG. ECARs were calculated using the preloaded Seahorse analyzer software.

### 2.8 Enzyme-Linked Immunosorbent Assay (ELISA)

Following the collection process, plasma was subjected to centrifugation at a speed of 3000 rotations per minute (rpm) for a duration of 15 minutes to facilitate the estimation of biochemical parameters. ANP and BNP were detected in the plasma using an enzyme-linked immunosorbent assay (ELISA) kit (ANP: #SEA225Mu; BNP: #SEA541Mu, Cloud-Clone Corp), as per the instructions provided by Cloud-Clone Corp.

### 2.9 Histological Analysis

After being immersed in 4% paraformaldehyde for a duration of 72 hours, the heart tissues were fixed. Subsequently, the tissues were embedded in paraffin and sectioned into 4 μm thick pieces. Then, these sections were subjected to Masson staining. For immunofluorescence (IF) analysis, sections were incubated with LYVE1 (#ab218535, Abcam, Cambridge, MA, USA), Prox1 (#ab199359, Abcam), and CD68 (#ab283654, Abcam) at 4 °C for 12 hours, and subsequently incubated with anti-Rabbit HRP (Alexa Fluor 647) and anti-Mouse HRP (Alexa Fluor 488) at 37 °C for 2 hours. After washing with PBS, the sections were counterstained with DAPI. The sections were examined using a fluorescence microscope and a digital camera (3DHistech, Budapest, Hungary).

### 2.10 Quantitative Real-Time Polymerase Chain Reaction (RT-PCR)

According to the guidelines provided by the manufacturer (Roche, Basle, Switzerland), mRNA reverse transcription was conducted using the mRNA reverse transcription kit to generate cDNA. RT-PCR was conducted by

a CFX96™ PCR detection system (BioRad, Redmond, WA, USA) using the SYBR Green PCR master mix (Roche). GAPDH and U87 were employed as internal reference genes for normalization purposes. All used primer sequences are provided below. *GAPDH* forward: TGTGTCCGTCGTGGATCTGA; reverse: CCTGCTTCACACCTTCTTG. *U87* forward: ACAATGATGACTTATGTTTT; reverse: GCTCAGTCTTAAGATTCTCT. *IL-1β* forward: TGTGCTCTGCTTGTGAGGTGCTG; reverse: GCCGTGGTTGGAGAGATAGG. *IL-6* forward: TAGTCCTTCTACCCCAATTTCC; reverse: TTGGTCTTAGCCACTCCTTC. *TNF-α* forward: GGTGATCGTCCCCAAAGGGATGA; reverse: TGGTTTGCTACGACGTGGGCT. *PKM2* forward: GTGGAGATGCTGAAGGAGATG; reverse: CAACAGGACGGTAGA-GAATGG. *GLUT1* forward: CGTCGTTGGCATCCTTATTG; reverse: CTCTTCAGCACACTCTTGG. *PFKFB3* forward: TGGTTGTATCAGTGAAGGAAGG; reverse: GGAAGGAAGGAAGGAAGGAAGG. *PFKFB2* forward: GGCAACATCCTCGT-TATCTC; reverse: GTCTACAGCATCCACATTTCAG. *HK2* forward: TGCGAATATGGTTGCCTCATCTTG; reverse: CTCTCCTCCTCCTCCTCTTCC. *VEGF-C* forward: CCGCTGTGTCCCATCGTATTG; reverse: AGTCCTCTCCCGCAGTAATCC. *VEGF-D* forward: AGTTATAGATGAAGAATGGCAGAG; reverse: CTTGAAGAATGTGTTGGTTGTC. *Pdpn* forward: CACCTCAGCAACCTCAGACC; reverse: TAACAAGACGCCAACTATGATTCC. *CcL21a* forward: CTGCTTCAACCATCACATCTG; reverse: GCTGTCTCCTCCTCATTCC.

### 2.11 Statistical Analysis

The data were analyzed using SAS statistical software (v9.4, SAS Institute, Cary, NC, USA). The mean ± standard deviation (SD) was used to present all quantitative data in this study. Pairwise comparisons were conducted using two-tailed Student's *t*-tests. To compare differences across multiple groups with a single variable, a one-way analysis of variance (ANOVA) was performed. A *p* value < 0.05 was considered statistically significant. The figure legends contain all numerical data pertaining to the experiments conducted.

## 3. Results

### 3.1 Promoting Lymphatic Regeneration is Beneficial for Heart Repair after I/R

In this research, we utilized intramyocardial injections of adeno-associated viruses (AAV9) to inhibit (*VEGFR3* shRNA) or promote the expression of *VEGFR3* (*VEGFR3* ORF) in the heart. Moreover, to serve as the control groups, AAV9-empty vectors were injected into the myocardium of the sham, I/R, and MAZ51 (a *VEGFR3* tyrosine kinase inhibitor that selectively hinders the activation of *VEGFR3* caused by *VEGF-C*) groups. To establish a model of is-

chemic heart failure (HF), the approach of subjecting the heart to 1 hour of cardiac ischemia followed by 14 days of reperfusion (I/R) was employed (Fig. 1A). Cardiac ultrasound was performed to assess the cardiac function of each experimental cohort (Fig. 1B–D). The M-mode pattern of the cardiac ultrasound, which served as a representative, indicated that the state of the left ventricular wall motion was considerably diminished in both the MAZ51 intervention and the *VEGFR3* shRNA groups, in contrast to the I/R group. Conversely, the *VEGFR3* ORF group significantly improved the state of the left ventricular wall motion following I/R (Fig. 1B). The measurement outcomes of the left ventricular ejection fraction (Fig. 1C, EF%) and short axis shortening rate (Fig. 1D, FS%) demonstrated a consistent trend; notwithstanding the reduction in MAZ51 and *VEGFR3* shRNA, where no significant difference was observed, while *VEGFR3* ORF displayed a noteworthy augmentation. In contrast to the I/R group, the degree of cardiac fibrosis in mice subjected to I/R and treated with MAZ51 and *VEGFR3* shRNA exhibited a significant increase. Conversely, *VEGFR3* ORF was found to notably ameliorate cardiac fibrosis in mice (Fig. 1E,F). Therefore, to evaluate lymphatic neogenesis in the heart of I/R mice in diverse experimental groups, immunofluorescence staining of lymphatic markers, such as lymphatic endothelial hyaluronic acid receptor 1 (*Lyve1*) and homeobox transcription factor 1 (*Prox1*), was employed. The results demonstrated that the interference of MAZ51 and *VEGFR3* shRNA had an adverse impact on the development of cardiac lymphatic vessels in mice that underwent I/R, whereas the administration of *VEGFR3* ORF demonstrated a marked improvement and facilitation of cardiac lymphatic neogenesis (Fig. 1G–I). The process of phagocytosis, in which macrophages engulf deceased cells, results in the transportation of cardiac antigens to the mediastinal lymph nodes (MLNs) [20]. In these nodes, the antigens may be presented to T cells, which are already present in the area, by a process known as cross-presentation [21]. Thus, to assess the impact of lymphangiogenesis on the drainage of myocardial cell debris towards the MLNs, an analysis was conducted on the level of cardiogenic (*Myh6*-mCherry) antigen present in the MLNs. The flow cytometry findings revealed that the number of cardiac mCherry antigens in the drained MLNs was significantly reduced upon inhibition of lymphangiogenesis (MAZ51 and *VEGFR3* shRNA), whereas promoting lymphangiogenesis significantly increased the aforementioned number (Fig. 1J,K). The mRNA expression of genes linked with lymphatic neogenesis, including *VEGFR3*, *VEGF-D*, podoplanin (*Pdpn*), and *Ccl21*, displayed coherence with the preceding results (Fig. 1L). Furthermore, the serum levels of ANP and BNP (Fig. 1M), which are markers of heart failure, indicated that hindering lymphangiogenesis through the use of MAZ51 and *VEGFR3* shRNA could considerably accelerate the advancement of the disease. Conversely, promoting lymphan-

giogenesis yielded contrasting outcomes. In conclusion, the promotion of lymphangiogenesis proved to be advantageous in the restoration of the heart following I/R.

### 3.2 *PFKFB3* Regulates the Production of *VEGF-C* by Macrophages

The ability to produce *VEGF-C* has been observed in cells that exhibit macrophage-like characteristics [7]. The current study employed *Lyz2<sup>Cre</sup> VEGF-C<sup>f1/f1</sup>* mice to abolish the expression of *VEGF-C* in macrophages, where *Lyz2* expression is evident in myeloid cell lines, such as monocytes and fully developed macrophages. The outcomes of immunofluorescence staining for *CD68* and *Lyve1* revealed that the ablation of *VEGF-C* expression in macrophages led to a significant decrease in the number of lymphatic vessels following I/R (Fig. 2A,B). The results obtained by flow cytometry analysis revealed that the ablation of *VEGF-C* expression in macrophages led to a marked increase in the number of macrophages present in the heart (Fig. 2C,D). Furthermore, it caused a significant elevation in the mRNA expression of inflammatory factors, such as *IL-1 $\beta$* , *IL-6*, and *TNF- $\alpha$* , in the heart (Fig. 2E). It has been established that the suppression of glycolysis could effectively impede the inflammatory reaction of macrophages [22,23]. However, the correlation between glycolysis inhibition and the production of *VEGF-C* by macrophages remains ambiguous. Notably, following I/R, there was an up-regulation in the expression of glycolytic-associated genes, including *PKM2*, *GLUT1*, *PFKFB3*, and *HK2*, within the cardiac macrophages, obtained by flow cytometry (FACS) (Fig. 2F). The glycolytic pressure test revealed a marked elevation in extracellular acidification rates (ECARs) post-I/R, indicating heightened glycolytic activity in cardiac macrophages following this event (Fig. 2G). In order to assess the impact of glycolysis inhibition on lymphatic neogenesis, we employed LPS to provoke inflammation and heighten glycolysis in bone marrow-derived macrophages (BMDM) of I/R mice [24]. Then, we utilized the *PFKFB3* inhibitor 3PO to intervene, as well as using adenovirus overexpression of *PFKFB3*. The outcomes demonstrated that the inhibition of *PFKFB3* had a significant impact on the glycolytic activity of BMDM, causing a decrease in its level (Fig. 2H). Moreover, the inhibition of *PFKFB3* led to a significant increase in the expression of *VEGF-C* and *VEGF-D* in BMDM (Fig. 2I). In addition, 3PO could reduce the glycolysis level of inactive macrophages (Fig. 2H) yet have no considerable influence on the expression of *VEGF-C* and *VEGF-D* (Fig. 2I). These results suggested that inhibiting the level of glycolysis in an activated state of macrophages can lead to an increase in the expression of *VEGF-C* and *VEGF-D*. Conversely, the overexpression of *PFKFB3* resulted in a significant increase in the glycolytic activity of BMDM (Fig. 2J), which was accompanied by a notable decrease in the expression of *VEGF-C* and *VEGF-D* (Fig. 2K). To summarize, the expression of *PFKFB3* in

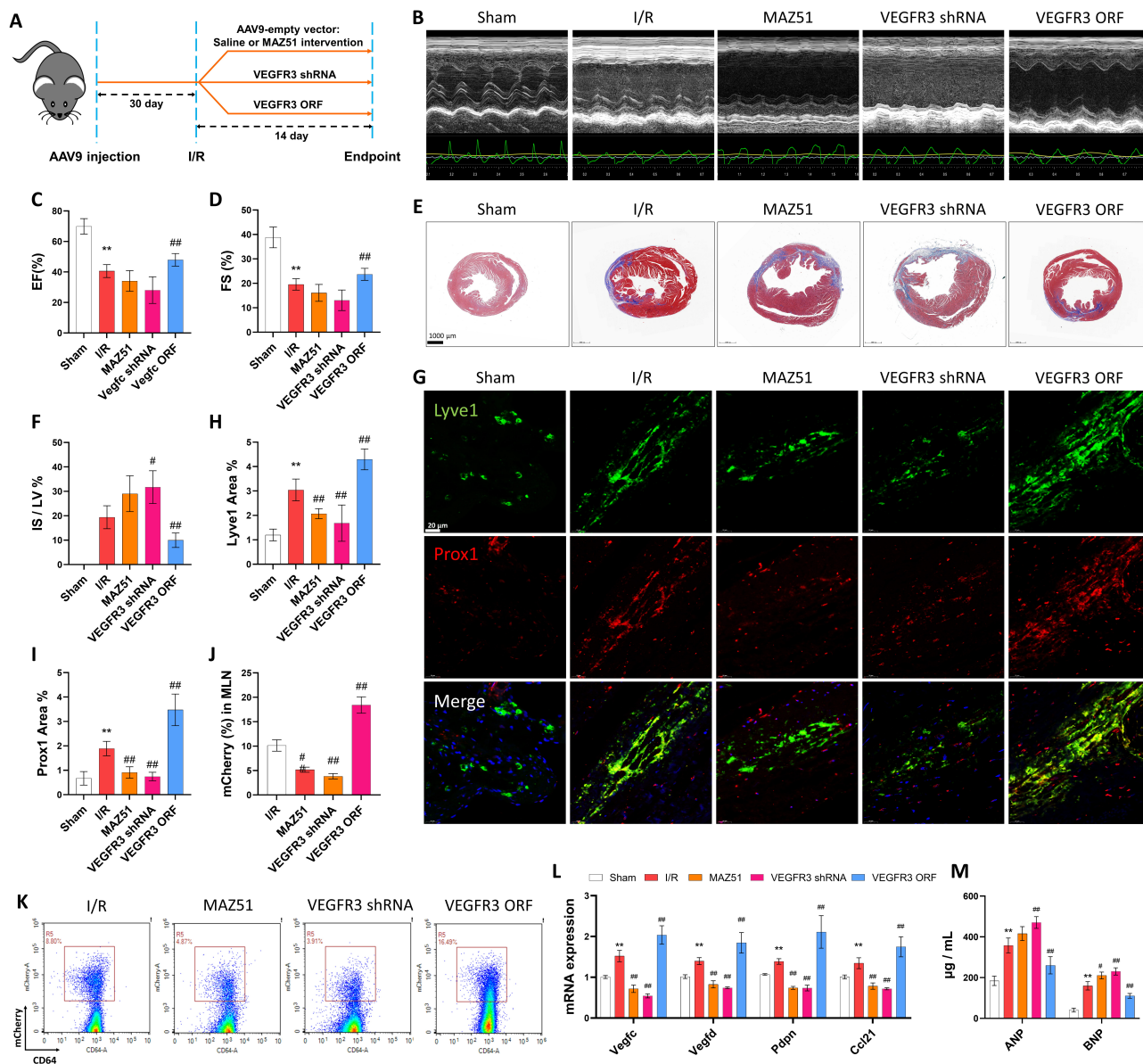


**Fig. 1. Promoting lymphatic regeneration is beneficial for heart repair after ischemia-reperfusion (I/R).** (A) Schematic overview of experimental procedure. (B) Representative image of M-mode in a cardiac ultrasound. Quantification of (C) EF% and (D) FS%, 14 days after I/R, data are presented as mean  $\pm$  SD of  $n = 8-10$  mice. (E-F) Representative Masson staining of heart transverse sections (scale bar = 1000  $\mu\text{m}$ ) and quantified IS/IV (infarct size: IS; left ventricular rate: LV, data are presented as mean  $\pm$  SD of  $n = 3$ ). (G-I) Representative immunostaining of *Lyve1* and *Prox1* in heart transverse sections (scale bar = 20  $\mu\text{m}$ ) and quantified *Lyve1* and *Prox1* area%, data are presented as mean  $\pm$  SD of  $n = 3$ . (J-K) MLNs were harvested, and flow cytometric analysis of  $\text{CD45}^+ \text{CD11b}^+ \text{CD64}^+ \text{mCherry}^+$  cells was performed, data are presented as mean  $\pm$  SD of  $n = 3$  mice. (L) The mRNA levels of *VEGF-C*, *VEGF-D*, podoplanin (*Pdpn*), and *Ccl21* in heart, data are presented as mean  $\pm$  SD of  $n = 3$  mice. (M) The mRNA expression of *VEGF-C*, *VEGF-D*, podoplanin (*Pdpn*), and *Ccl21*, data are presented as mean  $\pm$  SD of  $n = 6$  mice. (N) The levels of *ANP* and *BNP* in serum, data are presented as mean  $\pm$  SD of  $n = 6$  mice. Statistical significance is shown as: \*\* $p < 0.01$ , compared to the Sham group; # $p < 0.05$  and ### $p < 0.01$ , compared to the I/R group.

macrophages possesses a strong correlation with the production of *VEGF-C*. Moreover, it has been observed that hindering the function of *PFKFB3* could stimulate the generation of *VEGF-C*.

### 3.3 Elimination of Macrophage *PFKFB3* could Enhance Lymphangiogenesis Following I/R

In our study, we employed *Lyz2<sup>Cre</sup> PFKFB3<sup>f/f</sup>* mice to ablate the expression of *PFKFB3* in macrophages with the aim of investigating the impact of *PFKFB3* on

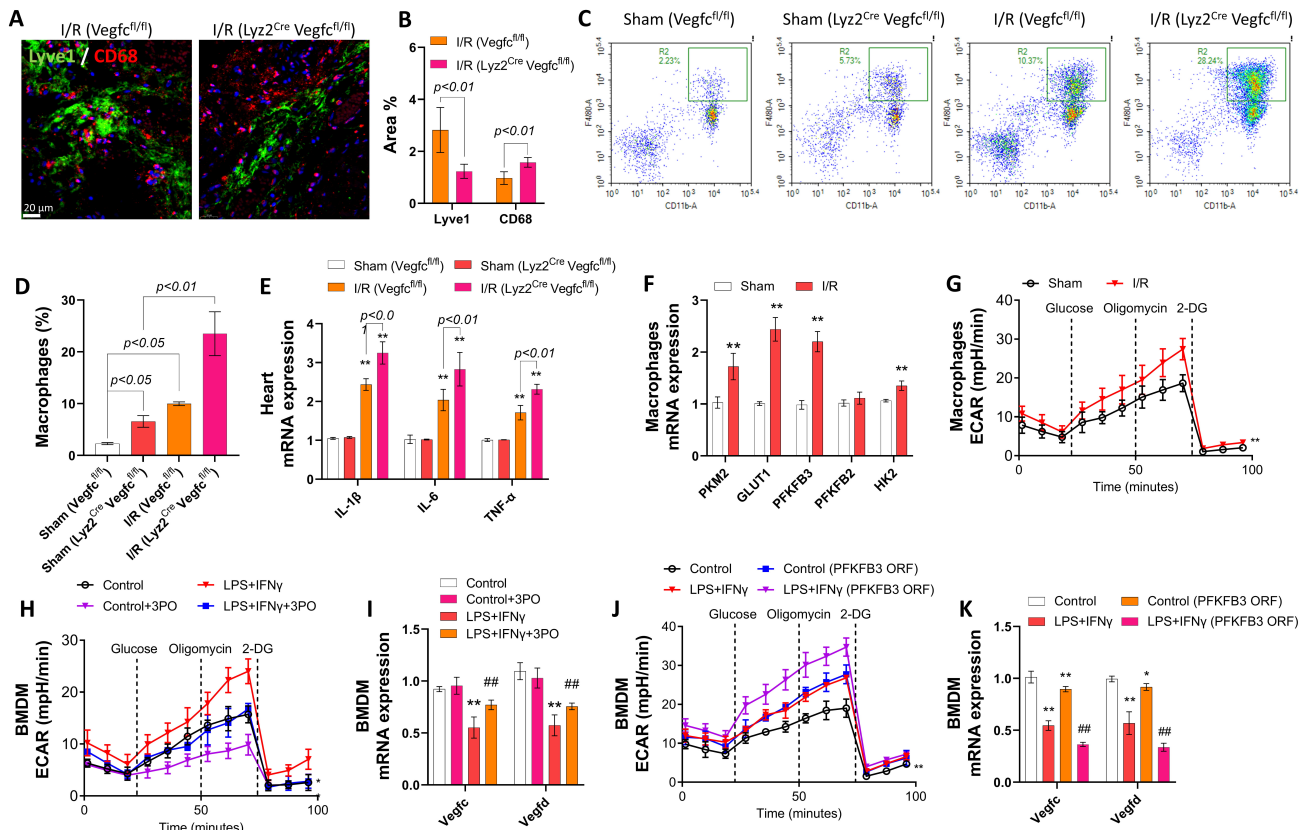


**Fig. 2. *PFKFB3* regulates the production of *VEGF-C* by macrophages.** (A–B) Representative immunostaining of *Lyve1* and *CD68* in heart transverse sections (scale bar = 20  $\mu$ m) and quantified *Lyve1* and *CD68* area%, data are presented as mean  $\pm$  SD of  $n = 3$ . (C–D) Flow cytometric analysis of  $CD11b^+ F4/80^+$  cells in the heart, data are presented as mean  $\pm$  SD of  $n = 3$  mice. (E) The mRNA levels of *IL-1 $\beta$* , *IL-6*, and *TNF- $\alpha$*  in the heart, data are presented as mean  $\pm$  SD of  $n = 3$  mice. (F) The mRNA levels of *PKM2*, *GLUT1*, *PFKFB3*, *PFKFB2*, and *HK2* in  $F4/80^+$  macrophages in the heart obtained by flow cytometry (FACS), data are presented as mean  $\pm$  SD of  $n = 3$  mice. (G) ECAR measurements in heart  $F4/80^+$  macrophages, as measured by Seahorse Bioscience XF96 analyzer,  $n = 3$ . (H,J) ECAR measurements in BMDMs of I/R mice, as measured by Seahorse Bioscience XF96 analyzer,  $n = 3$ . (I,K) The mRNA levels of *VEGF-C* and *VEGF-D* in BMDMs of I/R mice, data are presented as mean  $\pm$  SD of  $n = 3$  mice. Statistical significance is shown as: \* $p < 0.05$  and \*\* $p < 0.01$ , compared to the sham group; ### $p < 0.01$ , compared to the I/R group.

lymphatic neogenesis in the context of I/R. The findings of the cardiac ultrasound indicate that the inhibition of *PFKFB3* expression in macrophages could enhance the left ventricular wall motion in mice following I/R (Fig. 3A), leading to a notable improvement in ejection function (EF%) in mice with I/R (Fig. 3B). According to Mason's research, the inhibition of *PFKFB3* expression in macrophages could decrease the degree of cardiac fibrosis in I/R mice (Fig. 3C,D). Additionally, immunofluorescence staining of *Lyve1* and *Prox1* confirmed that this intervention resulted in an improvement in lymphatic neogenesis (Fig. 3E–G). The mRNA expressions of *VEGF-C*, *VEGF-D*, *Pdpn*, and *Ccl21* were significantly increased following the deletion of *PFKFB3* in mice subjected to I/R (Fig. 3H). Flow cytometry was employed to separate cardiac macrophages and qPCR was used to detect the mRNA expression of *VEGF-C*, *IL-1 $\beta$* , *IL-6*, and *TNF $\alpha$*  in cardiac macrophages. The results indicated that the expression of

*VEGF-C* in *PFKFB3*<sup>-/-</sup> cardiac macrophages was significantly higher than the *PFKFB3*<sup>f1/f1</sup> cardiac macrophages (Fig. 3I), and the mRNA expression of *IL-1 $\beta$* , *IL-6*, and *TNF $\alpha$*  in *PFKFB3*<sup>-/-</sup> cardiac macrophages was significantly lower than the *PFKFB3*<sup>f1/f1</sup> cardiac macrophages (Fig. 3J). The evidence gathered suggests that *PFKFB3* may have a role in modulating the lymphangiogenesis function during I/R injury.

### 3.4 Absence of *PFKFB3* in Macrophages Results in Improved Stability of Cardiac Immune Cells Post I/R

The quantification of neutrophils, monocytes, and macrophages in the heart following I/R was assessed through the utilization of flow cytometry (Fig. 4A–D). The findings indicated that the elimination of *PFKFB3* resulted in a substantial decrease in the population of neutrophils (Fig. 4B,E), monocytes (Fig. 4C,F), and macrophages (Fig. 4D,G) within the heart of mice undergoing I/R. Ad-

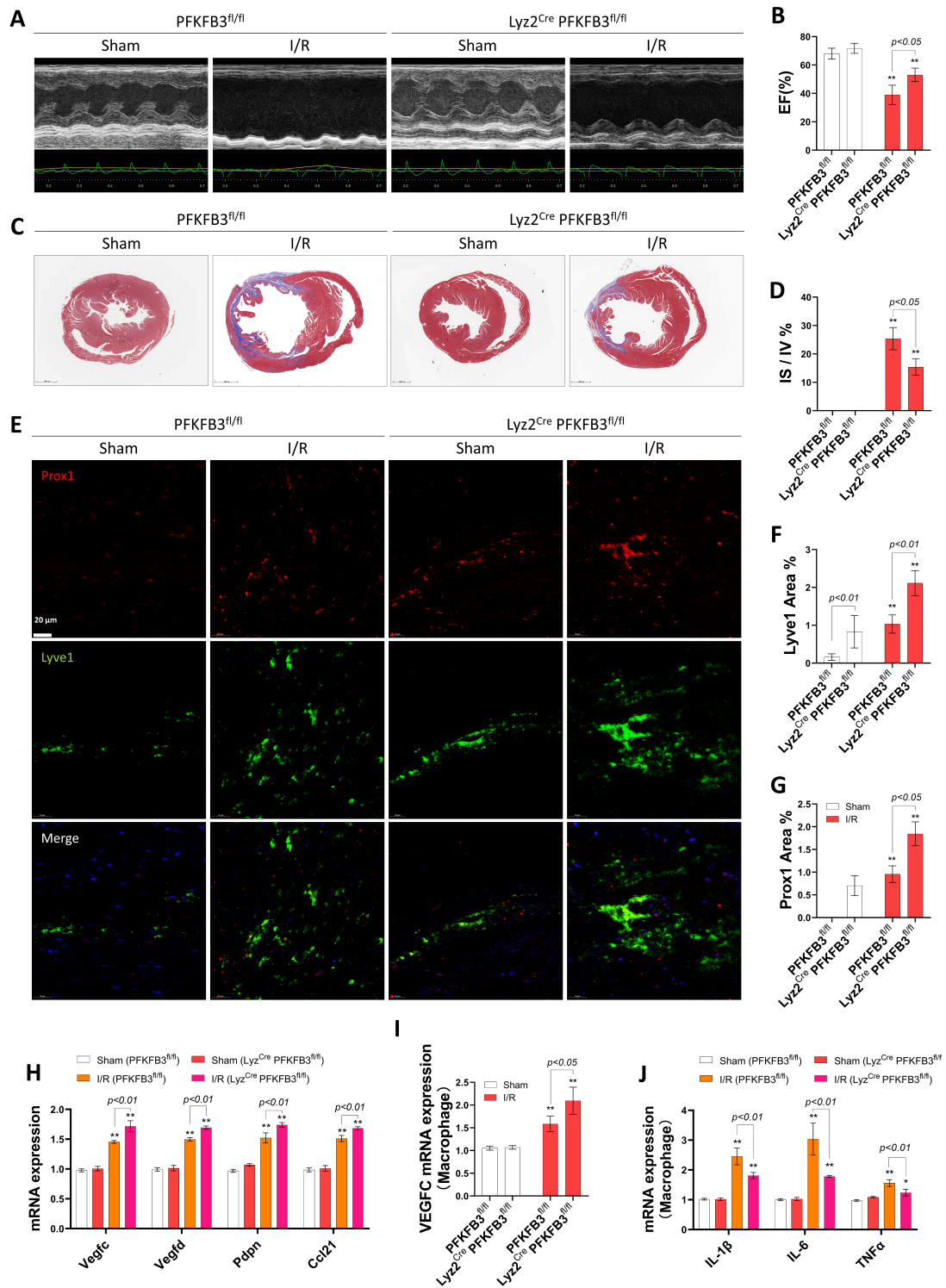


**Fig. 3. Elimination of *PFKFB3*-enhanced lymphangiogenesis following I/R.** (A) Representative image of M-mode in a cardiac ultrasound of *Lyz2<sup>Cre</sup> PFKFB3<sup>fl/fl</sup>* mice. Quantification of (B) EF% after I/R, data are presented as mean  $\pm$  SD of  $n = 6$  mice. (C,D) Representative Masson staining of heart transverse sections (scale bar = 1000  $\mu\text{m}$ ) and quantified IS/IV (infarct size: IS; left ventricular rate: LV, data are presented as mean  $\pm$  SD of  $n = 3$ ). (E–G) Representative immunostaining of *Lyve1* and *Prox1* in heart transverse sections (scale bar = 20  $\mu\text{m}$ ) and quantified LYVE1 and Prox1 area%, data are presented as mean  $\pm$  SD of  $n = 3$ . (H) The mRNA levels of heart *VEGF-C*, *VEGF-D*, podoplanin (*Pdpn*), and *Ccl21*, data are presented as mean  $\pm$  SD of  $n = 3$  mice. (I) The mRNA levels of *VEGF-C* in cardiac macrophages, data are presented as mean  $\pm$  SD of  $n = 3$  mice. (J) The mRNA levels of *IL-1 $\beta$* , *IL-6*, and *TNF $\alpha$*  in cardiac macrophages, data are presented as mean  $\pm$  SD of  $n = 3$  mice. Statistical significance is shown as: \* $p < 0.05$  and \*\* $p < 0.01$ , compared to the Sham group.

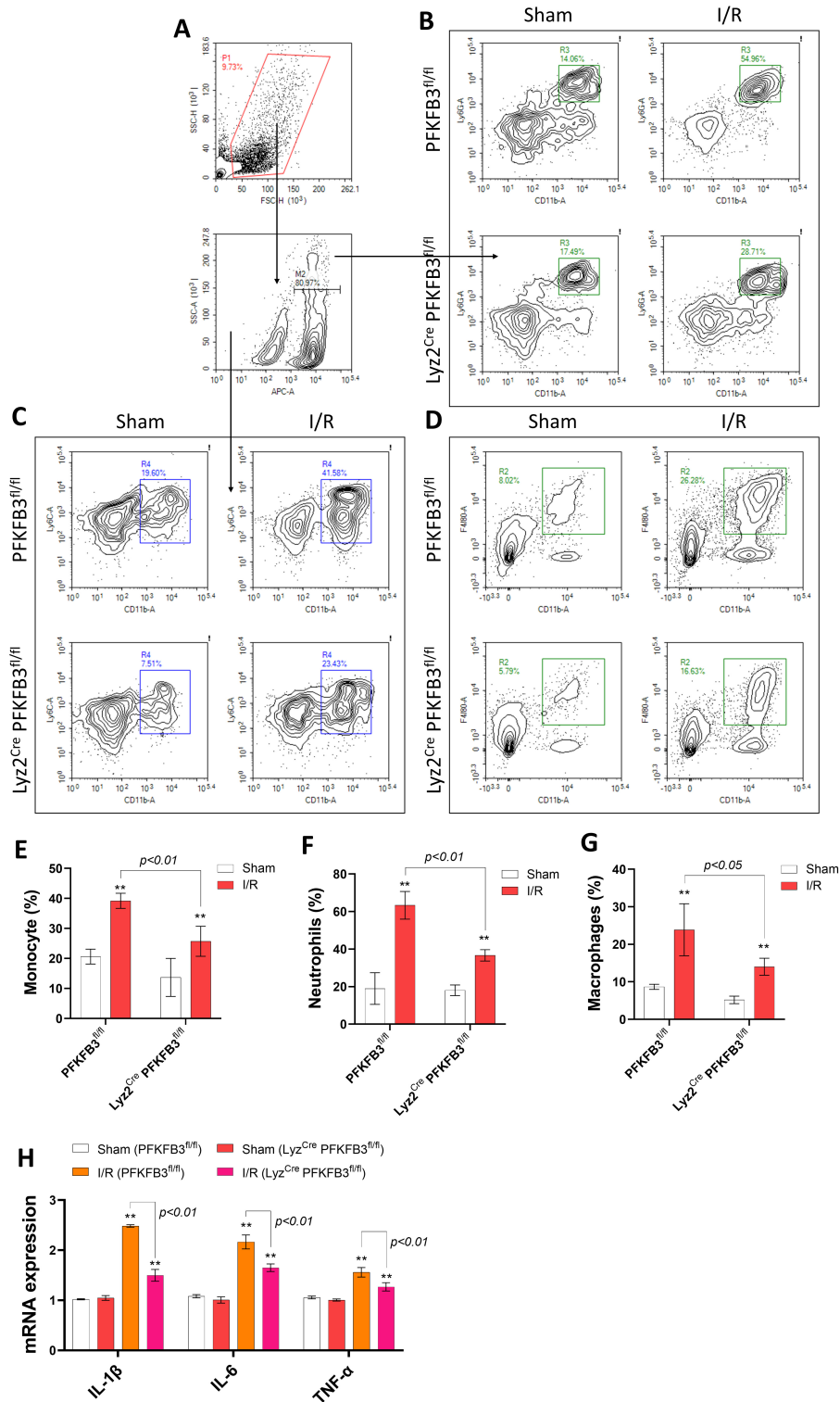


**Fig. 4. Absence of *PFKFB3* in macrophages results in improved stability of cardiac immune cells post I/R.** (A) Flow cytometric analysis of (B,E) neutrophils (CD11b<sup>+</sup> Ly6G<sup>+</sup>), (C,F) monocytes (CD11b<sup>+</sup> Ly6C<sup>high/low</sup>), and (D,G) macrophages in the heart (CD11b<sup>+</sup> F4/80<sup>+</sup>), data are presented as mean  $\pm$  SD of n = 3 mice. (H) The heart mRNA levels of *IL-1 $\beta$* , *IL-6*, and *TNF $\alpha$* , data are presented as mean  $\pm$  SD of n = 3 mice. Statistical significance is shown as: \*\*p < 0.01, compared to the Sham group.

ditionally, there was a significant reduction in the expression of inflammatory factors (*IL-1 $\beta$* , *IL-6*, and *TNF $\alpha$* ) in the

heart of *Lyz2<sup>Cre</sup> PFKFB3<sup>fl/fl</sup>* mice (Fig. 4H). In brief, our study has substantiated that the elimination of *PFKFB3* ex-

pression in macrophages could considerably augment I/R lymphangiogenesis, bolster the robustness of cardiac immune cells, and curtail the inflammatory reaction in the cardiac tissue.

#### 4. Discussion

It has been stated that the amplification of cardiac lymphangiogenesis post-myocardial infarction can enhance cardiac function [4,5]. The current investigation aims to establish a relationship between the aerobic glycolysis of macrophages and the expression of *VEGF-C*, which is stimulated by macrophages. Based on the initial findings, inhibiting the expression of *PFKFB3* in macrophages may enhance the generation of *VEGF-C* in macrophages, leading to the promotion of lymphatic neogenesis and the mitigation of the inflammatory response following I/R.

It has been previously established that the signal transduction of *VEGF-C/PFKFB3* plays a significant role in the regulation of lymphatic neogenesis [25]. The findings of our investigation indicate that impeding or suppressing the *VEGF-C/PFKFB3* signals leads to an upsurge in the progression of ventricular remodeling in response to I/R, while augmenting the expression of *VEGFR3* plays a salutary role in ameliorating ventricular remodeling after I/R. This process, which is advantageous for repairing the heart, is linked to the growth of lymphatic vessels. Upon the overexpression of *VEGFR3*, a noticeable increase in the quantity of cardiac antigens was observed in the MLNs. This observation suggests that the overexpression of *VEGFR3* facilitates the process of cardiac lymphangiogenesis, which in turn promotes the efficient flow of myocardial cell debris to the MLNs. The aforementioned procedure yields a reduction in the buildup of cellular waste in the cardiac muscle of individuals undergoing I/R, ultimately leading to a mitigation of inflammatory responses. Moreover, the *VEGF-C/VEGFR3* signaling pathway plays a crucial role in the modulation of macrophage plasticity [26]. Upon conducting our experiment, we noted an important induction in the mRNA expression of inflammatory factors in the cardiac region following the elimination of *VEGF-C* expression in *Lyz2<sup>+</sup>* cells. The rise in these inflammatory factors is generally thought to be connected to the activation of macrophages that belong to the M1 type. An upsurge in the number of macrophages was observed in the heart of I/R mice following the targeted removal of *VEGF-C* expression in *Lyz2<sup>+</sup>* cells. Regrettably, we did not conduct further analysis to determine the influence of *VEGF-C* in the transformation of cardiac macrophages from the M1 to M2 phenotype. As such, further investigations are imperative to gain a comprehensive understanding of the impact of *VEGF-C* on the orchestrated reorganization and operation of macrophages.

The general consensus is that M2-type macrophages, recognized for their anti-inflammatory attributes, are implicated in the restorative process of cardiac tissue following an injury [27]. The replacement of M1-type macrophages

with M2-type macrophages occurs within 7 to 14 days following an ischemia-reperfusion injury [28,29]. This transformation of a macrophage phenotype is closely associated with changes in their metabolic patterns. To be more precise, M1-type macrophages exhibit a greater reliance on the energy supply mechanism of glycolysis [23]. A hindrance to the glycolytic flow of macrophages is a contributing factor in the conversion of macrophages into the M2 type [23]. LPS has the ability to elicit a shift towards the M1 phenotype by macrophages [24], which is concomitant with a rise in glycolytic flux. During our experiment, we administered a glycolytic inhibitor, 3PO, to LPS-induced BMDM. The evidence gathered from our study indicates that the suppression of the glycolytic flux led to an increase in the expression of *VEGF-C* and *VEGF-D* in LPS-stimulated BMDM. This effect may be attributed to the facilitation of the DMBM transformation into a reparative phenotype.

The phagocytic activity of macrophages acts as a trigger for the upregulation of *VEGF-C* expression by macrophages in the context of tissue damage [30]. The findings of previous research have substantiated that *PFKFB2*-mediated glycolysis is capable of promoting sustained phagocytosis, which is driven by lactic acid in macrophages [24]. In contrast, the inhibition of phagocytosis is observed when macrophages silence *PFKFB2*. Although our experimental findings contradict this outcome, it is significant to note that the manner in which macrophage *PFKFB2* phosphorylation promotes an increase in phagocytosis is separate from the approach through which macrophage inflammation triggers glycolysis, as highlighted in this particular study [24]. In view of the adaptable and intricate nature of macrophages, particularly their diverse functions in the context of heart damage and recovery (whether it involves repair, injury, or both), it remains imperative to differentiate more precisely between the various subtypes of macrophages and their respective regulatory impacts on the formation of lymphangiogenesis following heart injury.

It is important to note that our experimental conclusions have limitations. The action of *Lyz2<sup>Cre</sup>* could also result in the removal of *PFKFB3* from both monocytes and granulocytes. Our study solely concentrated on the impact of the macrophage *PFKFB3* on lymphangiogenesis after 14 days of I/R, without taking into consideration its influence on lymphangiogenesis during the initial and intermediate stages following I/R. One must acknowledge the contrasting phenotypes and functions of macrophages during the early and middle stages of post-I/R compared to those at the 14-day mark. Furthermore, it is imperative to recognize the contribution of *VEGF-C* from alternative sources, such as vascular endothelial cells.

#### 5. Conclusions

Our initial investigations suggest that the suppression of *PFKFB3* expression in macrophages could potentially

stimulate the production of *VEGF-C* in these immune cells, which may facilitate lymphangiogenesis and mitigate the inflammatory effects of I/R injury.

### Availability of Data and Materials

The datasets used and/or analyzed during the current study are available from the corresponding author on reasonable request.

### Author Contributions

TC: Conceptualization, Methodology, Investigation, Writing — Original Draft, Visualization, Resources and Formal analysis; CF: Conceptualization, Methodology, Investigation, Writing — Original Draft, Visualization, Resources and Formal analysis; HJ: Conceptualization, Methodology, Investigation, Writing — Original Draft, Visualization, Resources and Formal analysis; YJ: Conceptualization, Methodology, Investigation, Writing — Original Draft, Visualization, Resources and Formal analysis; JF: Conceptualization, Methodology, Investigation, Writing — Original Draft, Visualization, Resources, Formal analysis, Project administration and Funding acquisition. All authors read and approved the final manuscript. All authors have participated sufficiently in the work and agreed to be accountable for all aspects of the work.

### Ethics Approval and Consent to Participate

All animal and surgical procedures conformed to Directive 2010/63/EU issued by the European Parliament. All animals were handled according to the guidelines of the TCM Animal Research Committee (TCM-LAEC2021409) of Tianjin University of Traditional Chinese Medicine.

### Acknowledgment

Not applicable.

### Funding

This research was funded by Tianjin Key Medical Discipline (Specialty) Construction Project; Tianjin Science and Technology Plan Project (21JCZDJC00600, JF); Tianjin Health Science and Technology Project (ZC20011, JF).

### Conflict of Interest

The authors declare no conflict of interest.

### References

- [1] Reed GW, Rossi JE, Cannon CP. Acute myocardial infarction. *Lancet*. 2017; 389: 197–210.
- [2] Roger VL, Weston SA, Redfield MM, Hellermann-Homan JP, Killian J, Yawn BP, *et al.* Trends in heart failure incidence and survival in a community-based population. *The Journal of the American Medical Association*. 2004; 292: 344–350.
- [3] Hausenloy DJ, Chilian W, Crea F, Davidson SM, Ferdinandy P, Garcia-Dorado D, *et al.* The coronary circulation in acute myocardial ischaemia/reperfusion injury: a target for cardioprotection. *Cardiovascular Research*. 2019; 115: 1143–1155.
- [4] Heron C, Dumesnil A, Houssari M, Renet S, Lemarcis T, Lebon A, *et al.* Regulation and impact of cardiac lymphangiogenesis in pressure-overload-induced heart failure. *Cardiovascular Research*. 2023; 119: 492–505.
- [5] Vieira JM, Norman S, Villa del Campo C, Cahill TJ, Barnette DN, Gunadasa-Rohling M, *et al.* The cardiac lymphatic system stimulates resolution of inflammation following myocardial infarction. *Journal of Clinical Investigation*. 2018; 128: 3402–3412.
- [6] Houssari M, Dumesnil A, Tardif V, Kivelä R, Pizzinat N, Boukhalifa I, *et al.* Lymphatic and Immune Cell Cross-Talk Regulates Cardiac Recovery after Experimental Myocardial Infarction. *Arteriosclerosis, Thrombosis, and Vascular Biology*. 2020; 40: 1722–1737.
- [7] Brakenhielm E, González A, Díez J. Role of Cardiac Lymphatics in Myocardial Edema and Fibrosis: JACC Review Topic of the Week. *Journal of the American College of Cardiology*. 2020; 76: 735–744.
- [8] Song L, Chen X, Swanson TA, LaViolette B, Pang J, Cunio T, *et al.* Lymphangiogenic therapy prevents cardiac dysfunction by ameliorating inflammation and hypertension. *eLife*. 2020; 9: e58376.
- [9] Beaini S, Saliba Y, Hajal J, Smayra V, Bakhos J, Joubran N, *et al.* VEGF-C attenuates renal damage in salt-sensitive hypertension. *Journal of Cellular Physiology*. 2019; 234: 9616–9630.
- [10] Liu Y, Xu R, Gu H, Zhang E, Qu J, Cao W, *et al.* Metabolic reprogramming in macrophage responses. *Biomarker Research*. 2021; 9: 1.
- [11] O'Neill LAJ, Hardie DG. Metabolism of inflammation limited by AMPK and pseudo-starvation. *Nature*. 2013; 493: 346–355.
- [12] Rider M, Bertrand L, Vertommen D, Michel S P, Rousseau G, Hue L. 6-Phosphofructo-2-kinase/fructose-2,6-bisphosphatase: head-to-head with a bifunctional enzyme that controls glycolysis. *Biochemical Journal*. 2004; 381: 561–579.
- [13] Li L, Wang Y, Guo R, Li S, Ni J, Gao S, *et al.* Ginsenoside Rg3-loaded, reactive oxygen species-responsive polymeric nanoparticles for alleviating myocardial ischemia-reperfusion injury. *Journal of Controlled Release*. 2020; 317: 259–272.
- [14] Zou Y, Li L, Li Y, Chen S, Xie X, Jin X, *et al.* Restoring Cardiac Functions after Myocardial Infarction-Ischemia/Reperfusion via an Exosome Anchoring Conductive Hydrogel. *ACS Applied Materials & Interfaces*. 2021; 13: 56892–56908.
- [15] Benedito R, Rocha SF, Woeste M, Zamykal M, Radtke F, Casanovas O, *et al.* Notch-dependent VEGFR3 upregulation allows angiogenesis without VEGF-VEGFR2 signalling. *Nature*. 2012; 484: 110–114.
- [16] Hsu M, Rayasam A, Kijak JA, Choi YH, Harding JS, Marcus SA, *et al.* Neuroinflammation-induced lymphangiogenesis near the cribriform plate contributes to drainage of CNS-derived antigens and immune cells. *Nature Communications*. 2019; 10: 229.
- [17] Ying W, Riopel M, Bandyopadhyay G, Dong Y, Birmingham A, Seo JB, *et al.* Adipose Tissue Macrophage-Derived Exosomal miRNAs can Modulate *in Vivo* and *in Vitro* Insulin Sensitivity. *Cell*. 2017; 171: 372–384.e12.
- [18] Ying W, Gao H, Dos Reis FCG, Bandyopadhyay G, Ofrecio JM, Luo Z, *et al.* MiR-690, an exosomal-derived miRNA from M2-polarized macrophages, improves insulin sensitivity in obese mice. *Cell Metabolism*. 2021; 33: 781–790.e5.
- [19] Li L, Ni J, Li M, Chen J, Han L, Zhu Y, *et al.* Ginsenoside Rg3 micelles mitigate doxorubicin-induced cardiotoxicity and enhance its anticancer efficacy. *Drug Delivery*. 2017; 24: 1617–1630.
- [20] Asano K, Nabeyama A, Miyake Y, Qiu C, Kurita A, Tomura M, *et al.* CD169-Positive Macrophages Dominate Antitumor Immunity by Crosspresenting Dead Cell-Associated Antigens. *Immunity*. 2011; 34: 85–95.

- [21] Hofmann U, Beyersdorf N, Weirather J, Podolskaya A, Bauersachs J, Ertl G, et al. Activation of CD4<sup>+</sup> T lymphocytes improves wound healing and survival after experimental myocardial infarction in mice. *Circulation*. 2012; 125: 1652–1663.
- [22] Mouton AJ, DeLeon-Pennell KY, Rivera Gonzalez OJ, Flynn ER, Freeman TC, Saucerman JJ, et al. Mapping macrophage polarization over the myocardial infarction time continuum. *Basic Research in Cardiology*. 2018; 113: 26.
- [23] Watanabe R, Hilhorst M, Zhang H, Zeisbrich M, Berry GJ, Wallis BB, et al. Glucose metabolism controls disease-specific signatures of macrophage effector functions. *JCI Insight*. 2018; 3: e123047.
- [24] Schilperoort M, Ngai D, Katerelos M, Power DA, Tabas I. PFKFB2-mediated glycolysis promotes lactate-driven continual efferocytosis by macrophages. *Nature metabolism*. 2023; 5: 431–444.
- [25] Harrison MR, Feng X, Mo G, Aguayo A, Villafuerte J, Yoshida T, et al. Late developing cardiac lymphatic vasculature supports adult zebrafish heart function and regeneration. *eLife*. 2019; 8: e42762.
- [26] Yamashita M, Niisato M, Kawasaki Y, Karaman S, Robciuc MR, Shibata Y, et al. VEGF-C/VEGFR-3 signalling in macrophages ameliorates acute lung injury. *European Respiratory Journal*. 2022; 59: 2100880.
- [27] Shiraishi M, Shintani Y, Shintani Y, Ishida H, Saba R, Yamaguchi A, et al. Alternatively activated macrophages determine repair of the infarcted adult murine heart. *Journal of Clinical Investigation*. 2016; 126: 2151–2166.
- [28] Yan X, Anzai A, Katsumata Y, Matsuhashi T, Ito K, Endo J, et al. Temporal dynamics of cardiac immune cell accumulation following acute myocardial infarction. *Journal of Molecular and Cellular Cardiology*. 2013; 62: 24–35.
- [29] Gao S, Li L, Li L, Ni J, Guo R, Mao J, et al. Effects of the combination of tanshinone IIA and puerarin on cardiac function and inflammatory response in myocardial ischemia mice. *Journal of Molecular and Cellular Cardiology*. 2019; 137: 59–70.
- [30] Glinton KE, Ma W, Lantz C, Grigoryeva LS, DeBerge M, Liu X, et al. Macrophage-produced VEGFC is induced by efferocytosis to ameliorate cardiac injury and inflammation. *Journal of Clinical Investigation*. 2022; 132: e140685.